

Creep Behavior of 9% Ni Alloy Steel at Elevated Temperatures

Chang-Min Suh* and Sang-Yeob Oh**

*School of Mechanical Engineering, Kyungpook National University, Daegu, Korea

**School of Automotive Engineering, Kyungpook National University, Sangju, Korea

KEY WORDS: Creep, Elevated temperature, Larson-Miller parameter, Life prediction, Activation energy

ABSTRACT: Little design data is available for the creep life prediction of 9% Ni alloy in elevated temperatures. Therefore, in this study, a series of creep tests under 16 combined conditions with 4 kinds of stresses and 4 temperatures was performed to obtain creep design and life prediction data for 9% Ni alloy, with the following results. The stress exponents decreased as the test temperature increased. The creep activation energy gradually decreased as the stresses became larger. The Larson-Miller parameter (LMP) constant for this alloy was estimated to be about 2.

1. Introduction

Most of the industrial facilities and their parts are used in high temperature and high pressure. Their conditions of application environment are to be worse gradually in order to maximize the performance. Therefore, it is important to develop a high temperature material. Especially, the decision and comprehension of an allowable stress for design is also very important in a point of view of the safety.

The 9% Ni alloy steel has been used as a material for a ground type of LNG tank. This material has a high toughness and good performance at a low temperature. This material mainly imported until few years ago, but recently it was developed by POSCO. Thus 9% Ni alloy steel is executed a series of creep tests for applying it at elevated temperature. Creep and fatigue tests are mainly studied for alloys and austenite stainless steels(Baek et al., 1994; Baek et al., 2000; Suh et al. 1988; Dorn, 1956). But the research of the nickel alloy is insufficient.

2. Experimental procedures

The creep deformation can be progressed by heat energy, which the deformation rate could be expressed by the Arrhenius's equation (ASM Metals handbook, 1985).

Currently, the activation energy of a creep process at the high temperature over 0.4~0.5 T_m (T_m : melting temperature) is well known to be the same as the activation energy of a self-diffusion in the case of a pure metal or a solid solution metal. This is expressed by Eq. (1).

$$\dot{\epsilon} = K \times \exp\left(-\frac{Q_{SD}}{RT}\right) \quad (1)$$

where $\dot{\epsilon}$ is the creep rate, Q_{SD} is the activation energy, R is the gas constant, T is the absolute temperature and K is the constant.

Firstly, a creep fracture test is performed to obtain the relation between stress and rupture time at a constant temperature of an original material for an estimating lifetime, respectively. In this study, Larson-Miller parameter curves are obtained, and two curves are plotted at the same graph. In order to estimate the residual lifetime from a stress, P_0 and P_1 are obtained by Eq. (2) and Eq. (3), respectively. The temperature is assumed an equivalent temperature T_{eq} because we don't know the exact temperature.

$$P_0 = T_{eq}(C + \text{Log}t_0) = T_{eq}[C + \text{Log}(t_1 + t)] \quad (2)$$

$$P_1 = T_{eq}(C + \text{Log}t_1) \quad (3)$$

where t is the used time, t_1 is the residual lifetime, and t_0 is the total lifetime.

In this study, the creep specimens of 9% Ni alloy steel is made by electric discharge machine (EDM) according to the KSB 0814 and ASTM No. 7 (ASM Metals handbook, 1985). Thereafter, it is annealed that cooling in furnace with holding time of 1 hour at 1020°C. Figure 1 shows the shape of the specimen.

The temperatures for the creep test are 380, 420, 460 and 500°C. And applied stresses are 200, 240, 280 and 320 MPa. The creep tests were carried out at 16 test conditions, respectively.

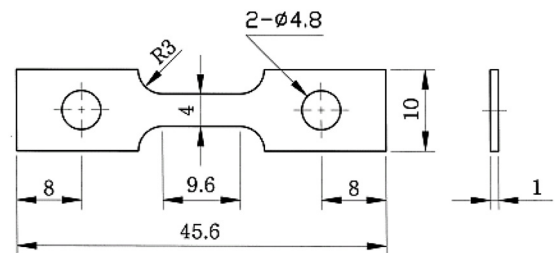


Fig. 1 Dimension of tensile creep specimen (unit: mm)

During uniform static load is loaded, a rupture time (t_r), a rupture strain (ϵ_r), and a minimum creep rate ($\dot{\epsilon}_{min}$) are measured experimentally. The effective life and the design allowable load can be obtained by these data.

Table 1 and Table 2 show chemical components and mechanical properties of 9% Ni alloy steel used in this study, respectively. This specimen is the material used in LNG storage tank facilities (KOGAS in Pyung-Taek).

The creep test apparatus in this study shown in Fig. 2 is a lever beam type. This apparatus can uniformly maintain a stress condition irrespective of the amount of the creep process. The ratio between the lever and arm is 1:15 for the cam lever type. An electrical furnace is used and its temperature is controlled by the temperature and power automatic control system. In addition, a specimen is set up within the quartz tube of the furnace in order to maintain the temperature within $\pm 1^\circ\text{C}$.

Table 1 Chemical composition of 9% Ni alloy steel (wt.%)

C	Si	Mn	P	S	Ni	Fe
0.038	0.235	0.589	0.003	0.0006	9.049	Bal.

Table 2 Mechanical properties of 9% Ni alloy steel

Yield Strength (MPa)	585
Ultimate Tensile Strength (MPa)	690
Elongation (%)	36
Min. impact value (J/-196°C)	70

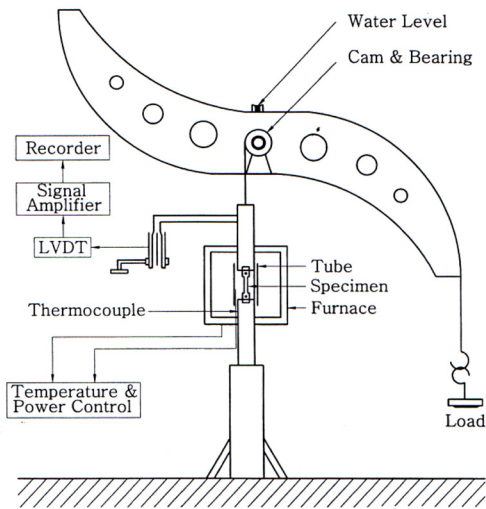


Fig. 2 Schematic diagram of the creep tester

The specimen is loaded after two hours holding time until the deformation rate is reached a constant level by the thermal expansion of the creep specimen.

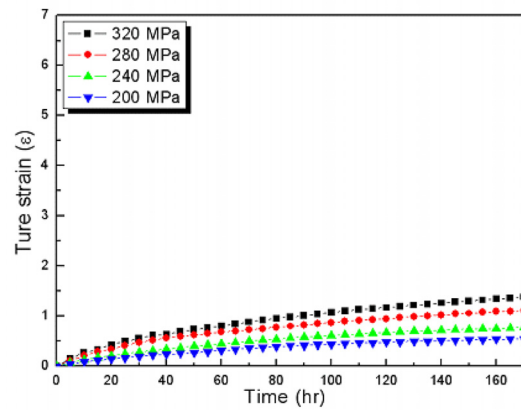
The length deformation of the specimen is measured by linear variable differential transformer (LVDT), (model: CAS-025) which can measure the deformation up to $\pm 1 \times 10^7 \mu\text{m}$. LVDT is attached on the steel plate in the back of the furnace which is not affected by heat and electromagnetism.

After performing the creep test at each test condition, the ruptured specimens are observed by a SEM (Model No. JSM-5600).

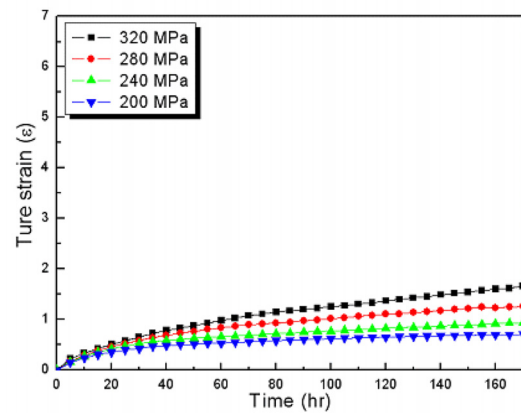
3. Results and discussion

3.1 Creep curve

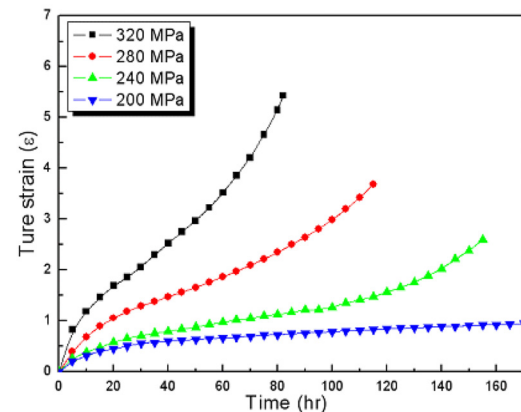
The creep curves are obtained by plotting the true strain ($\epsilon - \epsilon_0$) according to the displacement in the creep test, where ϵ are the total strain and ϵ_0 are the initial strain.



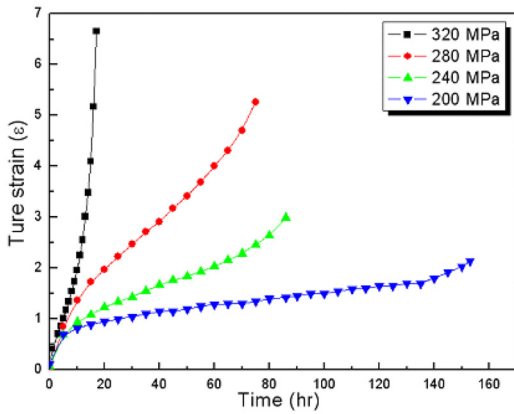
(a) 380°C



(b) 420°C



(c) 460°C



(d) 500°C

Fig. 3 Relation between the creep strain and the rupture time with 4 groups of temperature and stress level

Table 3 Experimental data for the creep test

Temp. (°C)	Stress (MPa)	Average creep rate, (hr ⁻¹)	Rupture time, <i>t_r</i> (hr)
380	200	0.00234	unfractured until 7 days
	240	0.00326	∕
	280	0.00438	∕
	320	0.00558	∕
420	200	0.00175	∕
	240	0.00262	∕
	280	0.00417	∕
	320	0.00587	∕
460	200	0.00265	∕
	240	0.00856	154
	280	0.02171	115
	320	0.04570	82
500	200	0.00625	153
	240	0.02033	86
	280	0.05075	75
	320	0.30900	17

The steady-state creep rate is calculated by Eq. (4).

$$\dot{\epsilon}_s = \frac{\epsilon_2 - \epsilon_1}{t_2 - t_1} \quad (4)$$

Table 3 shows experimental data including steady-state creep rate and rupture time at each temperature and stress level.

Figure 3 (a) and Figure 3 (b) show the creep curves measured at 380 and 420°C, respectively. In this case, the creep curves show that the stage I is very short and the stage II is very long. Under the given conditions, the specimens are not ruptured during 168 hours (7 days) at 4 groups of stress level from 200 to 320 MPa.

Figure 3 (c) shows the creep curves at 460°C. The minimum fracture time of the specimen is 82 hours and the maximum is 154 hours. Figure 3 (d) shows the creep curves measured at 500°C. The creep resistance and the fractured creep rate decrease as the stress level increases.

3.2 Time to rupture as the function of stress

Figure 4 indicates the relation between the rupture time (hr)

and the stress level (MPa) of 9% Ni alloy steel and Ni-5.8 Al-14.6Mo-6.2Ta single crystals for comparison (ASM Metals handbook, 1985). Two data of 9% Ni alloy and Ni-5.8Al-14.6 Mo-6.2Ta show different characteristics because of the difference of the material and testing conditions, that are, polycrystalline vs. single crystal, high stress level vs. low stress level and low temperature vs. high temperature. Two lines at 460°C and 500°C of 9% Ni alloy steel obtained from this study show slightly below the data of Ni-5.8Al-14.6Mo-6.2Ta.

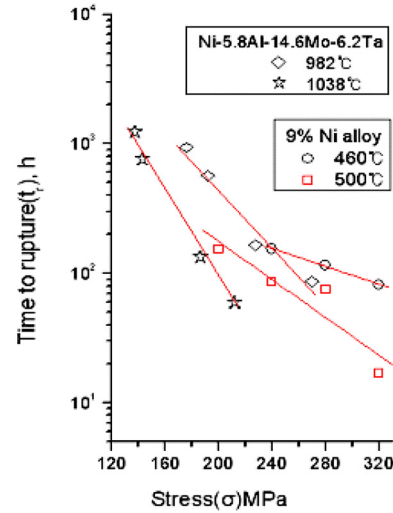


Fig. 4 Time to rupture as the function of stress for 9% Ni alloy steel compared with Ni-5.8Al-14.6Mo-6.2Ta (wt.%) single crystals [ASM Metals handbook, 1985]

3.3 Stress exponent for a creep rate

The creep process is that a deformation is continued with a time as the thermal activation process which a pure diffusion of atoms or gradual movement of dislocation for recovery is continued. In this creep process, the dependence of a stress level on the elevated temperature creep rate is expressed as Eq. (5) according to the studies of Garofalo (1965) and Cuddy (1970).

$$\dot{\epsilon}_s = K\sigma^n \quad (5)$$

where, σ is the stress level, $\dot{\epsilon}_s$ is the steady-state creep rate, K is the constant and n is the stress exponent.

Figure 5 shows an example of scatter band of steady-state creep rate at 420°C and the solid square marks indicate the average value of it.

Figure 6 shows the dependence of a creep rate $\dot{\epsilon}_s$ on an applied stress level σ from Eq. (5). It shows a linear relationship at each test temperature and the slope of this line is the stress exponent (n). As the creep test temperature increases from 380 to 500°C, the stress exponent gradually increases to 2.48, 4.94, 5.89, and 8.43 depending on the stress level, respectively.

The stress exponent increases as the temperature increases. This reason is that the dislocation density is decreased and the activation energy is also increased when the stress is going up. The similar results of these were also obtained in other

studies (Garofalo et al., 1962; Garofalo, 1965; Cuddy, 1970).

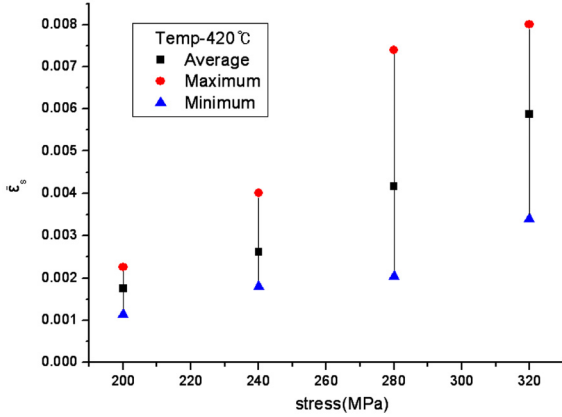


Fig. 5 An example of scatter band of steady-state creep rate at 420°C and solid square marks indicate the average value of it

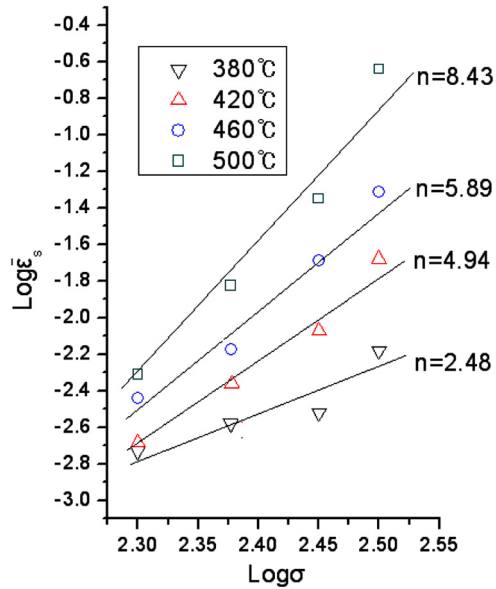


Fig. 6 Dependence of a creep rate on an applied stress level

3.4 The activation energy for a creep rate

The creep rate is controlled by a thermal activation process, so it can be expressed as the Arrhenius-type Eq. (6).

$$\dot{\epsilon}_s = K \times \exp\left(-\frac{Q_c}{RT}\right) \quad (6)$$

where, Q_c is the activation energy for the creep process, K is the constant for stress, microstructure and temperature, R is the gas constant and T is the absolute temperature.

Figure 7 shows the dependence of a creep rate $\dot{\epsilon}_s$ on an applied stress level σ and $1/T$ (reciprocal of temperature).

From this equation, Q_c can be obtained as the slope of $\ln \dot{\epsilon}_s$ and $1/T$. Therefore, Q_c is obtained from the slope of straight line as shown in Fig. 7. The activation energy for the creep process Q_c from this figure is obtained as 110.93, 218.94, 262.78, and 373.81 kJ/mol corresponding to the stress level

200, 240, 280, and 320 MPa, respectively.

The activation energy of the creep process is decreased with decreasing stress level. This phenomenon is described with Eq. (9) and Eq. (10) which are the relational equation of creep activation energy and effective stress as shown by Bradley, etc. (Bradley et al., 1976).

$$Q_c = Q_{SD} - \alpha_e (\Delta V) \quad (9)$$

$$\alpha_e = \alpha_a - \alpha_i \quad (10)$$

where, Q_c is the activation energy for a creep process, Q_{SD} is the activation energy for a self-diffusion, α_a is the applied stress, α_e is the effective stress, α_i is the internal stress, ΔV is the activation volume for a creep process.

α_e and ΔV increase according to α_a therefore, Q_c is seen to decrease with increasing α_e . According to Garofalo (Garofalo, 1965), if the creep temperature is about $0.5 T_m$, the activation energy for creep is nearly same to that for the self-diffusion. If the creep rate is low, the activation energy for creep is low too. Thus accompanied by the precipitation in alloy, the activation energy for creep is higher than that for the self-diffusion in the parent metal.

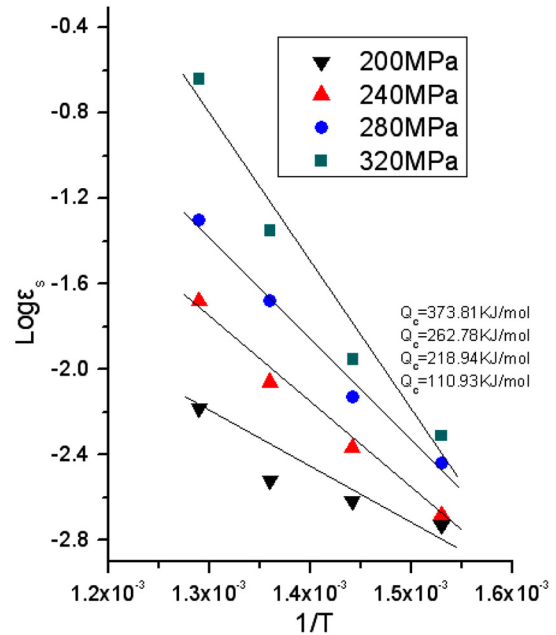


Fig. 7 Dependence of a creep rate on temperature and stress level

3.5 Prediction of a residual creep life

Table 3 shows the creep data and compares the rupture time of the material at the same temperature. The rupture life is decreased rapidly with increasing the external stress at 460°C and 500°C. Therefore, when the rupture life is known at some temperature region, the estimate methods of those at other temperature region can be done by the Larson-Miller parameter and the Manson-Haferd parameter (Manson and Haferd, 1953).

In this study, the Larson-Miller parameter as shown in Eq. (11)

is used, which is simple and widely applied to many alloys.

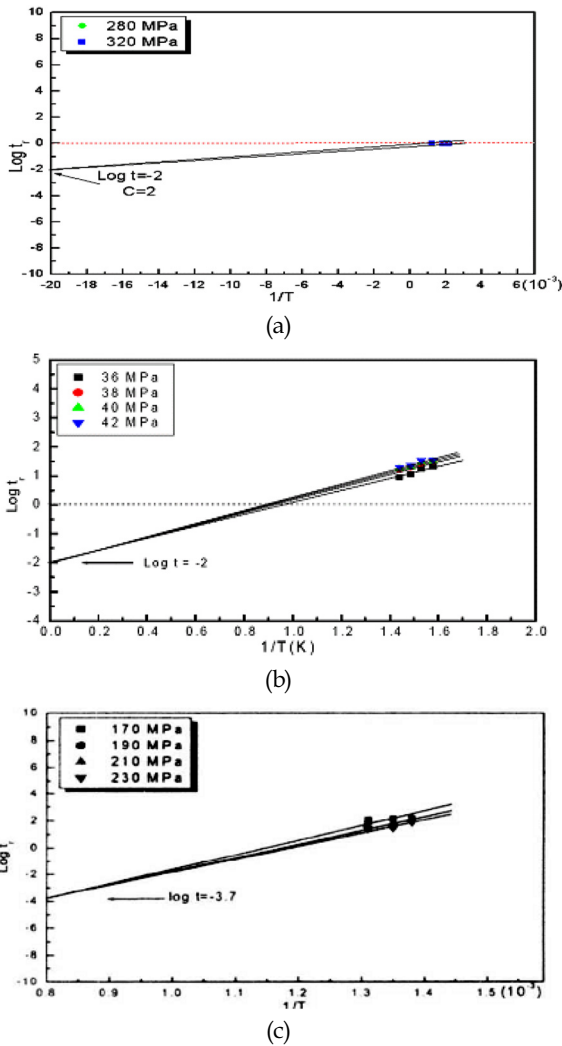


Fig. 8 Determination of the Larson-Miller parameter from stress-fracture time curves. (a) 9% Ni alloy steel. (b) Pure copper [Hwang et al. 2005] and (c) α -Ti alloy [Hwang and Yoon, 2004]

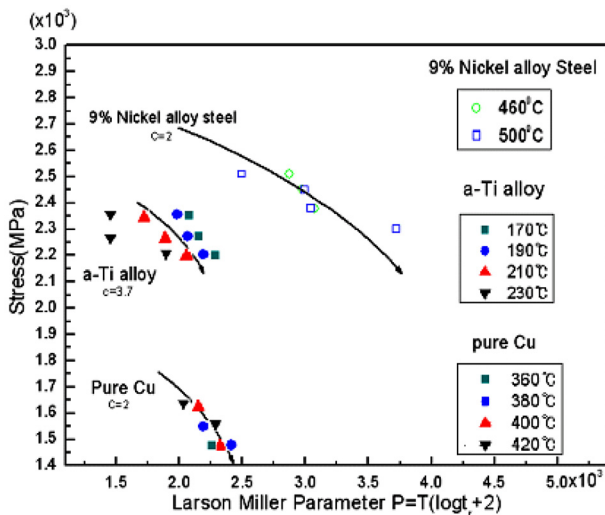


Fig. 9 Comparison of the Larson-Miller parameter for 9% Ni alloy steel, pure copper [Hwang et al. 2005] and α -Ti alloy [Hwang et al. 2004] by the experimental stress-rupture curves

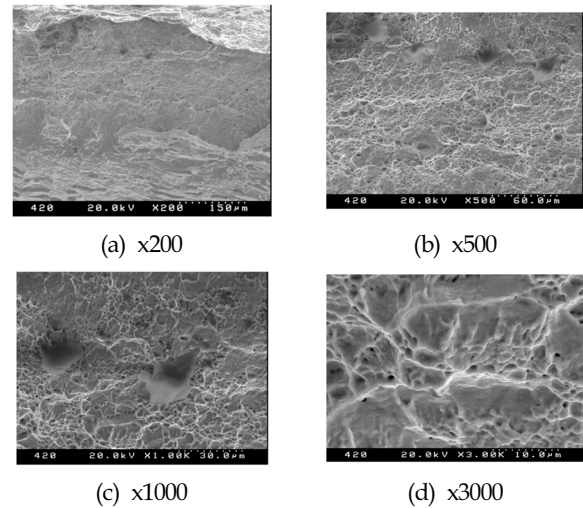


Fig. 10 SEM micrographs of the static creep rupture at temperature 460°C and stress level 320 MPa

$$P = f(\sigma) = T(\log t_r + C) \quad (11)$$

where, P is the Larson-Miller parameter, T is the absolute temperature, t_r is the rupture time, σ is the stress, and C is the constant.

The creep life can be estimated by the constant C from Eq. (11). Using the data in Table 3, C can be calculated by the extrapolation method for the correlation graph of $\log t_r$ and $1/T$, therefore the C is about 2 as shown in Fig. 8 (a). Two similar examples of determination of the Larson-Miller parameter from stress and fracture time curves of a pure copper and a α -Ti alloy were shown for comparison at Fig. 8 (b) and Fig. 8 (c), respectively [Hwang and Yoon, 2004; 2005].

Therefore, the Larson-Miller parameter of this study can be expressed as Eq. (12). Figure 9 shows the difference of the Larson-Miller parameter for 9% Ni alloy steel with pure copper and α -Ti alloy by the experimental stress-rupture curves (Larson and Miller, 1952).

$$P = T(\log t_r + 2) \quad (12)$$

3.6 Observation of a creep rupture surface

Generally, there are generally two reasons for the decrease of creep life. The first opinion is based on the damage of void that is generated and grown at the grain boundary during the creep process. The second opinion is the promotion of crack generation that is based on the effect of oxidation, although void is not generated at the grain boundary during the creep process. This test material is more considered as the first opinion.

Figure 10 shows SEM micrographs under the test condition of temperature 460°C and stress 320 MPa. When enlarged the microstructure of the fractured surface, the dimple is dominantly observed at plastic deformation is observed at Fig. 10 (a) and ductile fracture Fig. 10 (b, c, d). The phase of the ductile fracture is shown by the intergranular fracture because of elevated temperature and stress level.

4. Conclusions

9% Ni alloy steel which has a high ductility and a good performance at low temperature is creep-tested at elevated temperatures, that is, 4 groups of temperature are 380, 420, 460, and 500°C and that of stress is 200, 240, 280, and 320 MPa, respectively. Therefore the basic data is obtained in order to know the residual life of creep. The obtained results are as follows.

(1) The stress exponent (n) for the creep process was gradually increased to 2.48, 4.94, 5.89, and 8.43 with increasing the creep test temperature 380, 420, 460, and 500°C, respectively.

(2) The creep activation energy for the creep process (Q_c) was gradually increased as 110.93, 218.94, 262.78, and 373.81 kJ/mol with increasing of the stress 200, 240, 280, and 320 MPa, respectively.

(3) Creep life can be estimated and calculated by the extrapolation method for the correlation graph of $\log t_r$ and $1/T$, so that C is about 2.

References

- ASM Metals handbook (1985). 9th ed. Vol 8, pp 299-342.
- Baek, U.B. Nahm, S.H. Suh, C.M. and Yoon, K.B. (1994). "A Study on Initial Transient Behavior in Creep-Fatigue Crack Growth", Trans. of KSME, Vol 18, No 7, pp 1722-1729.
- Baek, U.B. Yoon, K.B. Lee, H.M. and Suh, C.M. (2000). "Creep-Fatigue Crack Growth at Cr-Mo Steel Weld Interface", Trans. of KSME, A, Vol 24, No 12, pp 3088-3095.
- Bradley, W.L. Nam, S.W. and Matlock, D.K. (1976). "Fatigue and Creep of Pure Aluminum at Ambient Temperatures", Met. Trans, 7A, pp 425-430.
- Cuddy, L.J. (1970). "Internal Stresses and Structures Developed during Creep", Met. Trans., Vol 1, pp 395-401.
- Dorn, J.E. (1956). "Creep and Fracture of Metals at High Temperatures", NPL Symposium, London, H.M.S.O. p 89.
- Garofalo, F. (1965). "Fundamentals of Creep and Creep Rupture in Metals", The Macmillan Co, New York. p 258.
- Garofalo, F. Richmond, O. and Domis, W.F. (1962). "Design of Apparatus for Constant Stress or Constant Load Creep Tests", J. of Basic Eng, June, pp 278-293.
- Hwang, K.C. and Yoon, J.H. (2004). "Creep Behaviors of α -Titanium Alloy, The Korean Society of Automotive Engineers", Proc. of Annual Autumn Conference, pp 68-75.
- Hwang, K.C. and Yoon, J.H. (2005). "Static Creep Behaviors of Pure Copper, The Korean Society of Automotive Engineers", Proc. of Annual Spring Conference, pp 950-956.
- Larson, F.R. and Miller, J. (1952). "A Time Temperature Relationship for Rupture and Creep stresses", Transaction of the ASME, pp 765-775.
- Manson, S.S. and Haferd, A.M. (1953). "A Linear Time-Temperature Relation for Extrapolation of Creep and Stress Rupture Data", NASA-TN-2890, National Aeronautics and Space Administration, March.
- Suh, C.M. Lee, S.D. and Cho, I.H. (1988). "Micro-Surface-Cracks Behavior of 304 Stainless Steel under Creep-Fatigue Interaction at Elevated Temperature", J. of Ocean Eng. and Technology, Vol 2, No 2 pp 304-311.

2010년 3월 5일 원고 접수

2010년 10월 11일 심사 완료

2011년 8월 16일 게재 확정